A minimum-norm current expansion method based on MT-BCS for inverting scattered data

L. Poli, G. Oliveri, F. Viani, A. Massa

Abstract

An innovative multi-step microwave imaging technique based on the multi-task Bayesian compressive sensing (MT–BCS) strategy is introduced in this report to image 2D-sparse dielectric profiles. The mathematical formulation of the minimum current approach is presented and some preliminary numerical results are proposed.

1 Mathematical Formulation

1.1 The Minimum Norm Current Approach

Let us consider an investigation domain of extension D illuminated by a set of V known incident transverse-magnetic waves whose electrical field is $E_v^{inc}(x,y)\hat{z}$. Inside the investigation domain are placed one or more scetterer objects, whose dielectric properties are modeled by means of the object function $\tau(x,y)$. Let us condider now the data equation:

$$E_v^{scatt}(x,y) = \int_D J_v(x',y')G_{2D}(x,y/x',y')dx'dy' \tag{1}$$

where $E_v^{scatt}(x,y)$ is the scattered field, $G_{2D}^{ext}(x,y/x',y')$ is the two-dimensional free-space Green's function, and $J_v(x',y')$ is the contrast source.

In matricial form we have

$$[E_v^{scatt}] = [G_{2D}^{ext}][J_v] \tag{2}$$

where

$$[E_v^{scatt}] = \begin{bmatrix} E_v^{scatt}(x_1,y_1) \\ ... \\ E_v^{scatt}(x_m,y_m) \\ ... \\ E_v^{scatt}(x_M,y_M) \end{bmatrix} \tag{3}$$

with size $M \times 1$, $m = 1,...,M$ and $v = 1,...,V$, where M is the number of measurement points and V is the number of views;

$$[G_{2D}^{ext}] = \begin{bmatrix} G_{2D}^{ext}(\rho_{11}) & ... & G_{2D}^{ext}(\rho_{1n}) & ... & G_{2D}^{ext}(\rho_{1N}) \\ ... & ... & ... & ... & ... \\ G_{2D}^{ext}(\rho_{m1}) & ... & G_{2D}^{ext}(\rho_{mn}) & ... & G_{2D}^{ext}(\rho_{mN}) \\ ... & ... & ... & ... & ... \\ G_{2D}^{ext}(\rho_{M1}) & ... & G_{2D}^{ext}(\rho_{Mn}) & ... & G_{2D}^{ext}(\rho_{MN}) \end{bmatrix} \tag{4}$$

with size $M \times N$, where N is the number of cells in the investigation domain, and $\rho_{mn} = \sqrt{\left[(x_m - x_n')^2 + (y_m - y_n')^2\right]}$.

$$[J_v] = \begin{bmatrix} J_v(x_1,y_1) \\ ... \\ J_v(x_n,y_n) \\ ... \\ J_v(x_N,y_N) \end{bmatrix} \tag{5}$$

with size $N \times 1$;

Applying the SVD to the matrix $G_{2D}^{ext}(x,y/x',y')$, we obtain:

$$[G_{2D}^{ext}] = [U][S][V]^{T*} \tag{6}$$

where

$$[U] = \begin{bmatrix} u_{11} & ... & u_{1m} & ... & u_{1M} \\ ... & ... & ... & ... & ... \\ u_{m1} & ... & u_{mm} & ... & u_{mM} \\ ... & ... & ... & ... & ... \\ u_{M1} & ... & u_{Mm} & ... & u_{MM} \end{bmatrix} \tag{7}$$

with size $M \times M$

$$[S] = \begin{cases} \begin{bmatrix} \sigma_{11} & 0 & 0 & 0 & 0 & 0 & ... & 0 \\ 0 & ... & 0 & 0 & 0 & 0 & ... & 0 \\ 0 & 0 & \sigma_{ii} & 0 & 0 & 0 & ... & 0 \\ 0 & 0 & 0 & ... & 0 & 0 & ... & 0 \\ 0 & 0 & 0 & 0 & \sigma_{II} & 0 & ... & 0 \end{bmatrix} & if\, M < N \\ \begin{bmatrix} \sigma_{11} & 0 & 0 & 0 & 0 \\ 0 & ... & 0 & 0 & 0 \\ 0 & 0 & \sigma_{ii} & 0 & 0 \\ 0 & 0 & 0 & ... & 0 \\ 0 & 0 & 0 & 0 & \sigma_{II} \end{bmatrix} & if\, M = N \\ \begin{bmatrix} \sigma_{11} & 0 & 0 & 0 & 0 \\ 0 & ... & 0 & 0 & 0 \\ 0 & 0 & \sigma_{ii} & 0 & 0 \\ 0 & 0 & 0 & ... & 0 \\ 0 & 0 & 0 & 0 & \sigma_{II} \\ 0 & 0 & 0 & 0 & 0 \\ ... & ... & ... & ... & ... \\ 0 & 0 & 0 & 0 & 0 \end{bmatrix} & if\, M > N \end{cases} \tag{8}$$

with size $M \times N$ and $I = Min\{M, N\}$,

$$[V] = \begin{bmatrix} v_{11} & ... & v_{1n} & ... & v_{1N} \\ ... & ... & ... & ... & ... \\ v_{n1} & ... & v_{nn} & ... & v_{nN} \\ ... & ... & ... & ... & ... \\ v_{N1} & ... & v_{Nn} & ... & v_{NN} \end{bmatrix} \tag{9}$$

with size $N \times N$.
We can define the basis minimum norm current

$$[B_v^{mn}] = [V]_{truncated} \tag{10}$$

where

$$[V]^{truncated} = \begin{bmatrix} v_{11} & ... & v_{1n} & ... & v_{1\rho} & 0 & ... & 0 \\ ... & ... & ... & ... & ... & 0 & ... & 0 \\ v_{n1} & ... & v_{nn} & ... & v_{n\rho} & 0 & ... & 0 \\ ... & ... & ... & ... & ... & 0 & ... & 0 \\ v_{N1} & ... & v_{Nn} & ... & v_{N\rho} & 0 & ... & 0 \end{bmatrix} \tag{11}$$

where $\rho = Rank\{[G_{2D}^{ext}]\}$. The related coefficients are

$$[A] = \begin{bmatrix} \alpha_1 \\ ... \\ \alpha_i \\ ... \\ \alpha_\rho \end{bmatrix} = [S_\rho]^{-1}[U]^{T*}[E_v^{scatt}] \tag{12}$$

where

$$[S_\rho] = \begin{bmatrix} \sigma_{11} & 0 & 0 & 0 & 0 \\ 0 & ... & 0 & 0 & 0 \\ 0 & 0 & \sigma_{ii} & 0 & 0 \\ 0 & 0 & 0 & ... & 0 \\ 0 & 0 & 0 & 0 & \sigma_{\rho\rho} \end{bmatrix} \tag{13}$$

Now, it is possible to estimate the minimum norm current as

$$[J_v^{mn}] = [B_v^{mn}][A] \tag{14}$$

1.2 Inverse CS Problem under the Minimum Norm Current Approach

Using Compressive Sampling techniques it is possible to solve linear problems such as: given $\overline{y} = \overline{A} \cdot \overline{x}$ find $\overline{x}$ such that $\overline{x} \in C^M$ and $\overline{x}$ is sparse. Considering the minimmum norm current approach, we can apply the multi-task bayesian compressive sampling technique (MT-BCS) exploiting the correlation the scattered fields generated by the real and imaginary parts of the minimum norm current J_v^{mn}. More in detail, using multi-task compressive sampling we can exploit the correlation between two linear problems of the kind

$$\begin{cases} \overline{y}' = \overline{A} \cdot \overline{x}' \\ \overline{y}'' = \overline{A} \cdot \overline{x}'' \end{cases} \tag{15}$$

In the specific case, we can decompose the *data* equation (1) into

$$\begin{cases} E_v^{scatt-re}(x,y) = \int_D G_{2D}(x,y/x',y')\mathrm{Re}\left\{J_v^{mn}(x',y')\right\} dx'dy' \\ E_v^{scatt-im}(x,y) = \int_D G_{2D}(x,y/x',y')\mathrm{Im}\left\{J_v^{mn}(x',y')\right\} dx'dy' \end{cases} \tag{16}$$

By expressing the formulation in matricial form, we have

$$\begin{cases} [E_v^{scatt-re}] = [G_{2D}^{ext}][\mathrm{Re}\left\{J_v^{mn}\right\}] \\ [E_v^{scatt-im}] = [G_{2D}^{ext}][\mathrm{Im}\left\{J_v^{mn}\right\}] \end{cases} \tag{17}$$

where

$$[E_v^{scatt-re}] = \begin{bmatrix} E_v^{scatt-re}(x_1,y_1) \\ \dots \\ E_v^{scatt-re}(x_m,y_m) \\ \dots \\ E_v^{scatt-re}(x_M,y_M) \end{bmatrix}, \quad [E_v^{scatt-im}] = \begin{bmatrix} E_v^{scatt-im}(x_1,y_1) \\ \dots \\ E_v^{scatt-im}(x_m,y_m) \\ \dots \\ E_v^{scatt-im}(x_M,y_M) \end{bmatrix} \tag{18}$$

with size $M \times 1$,

$$[G_{2D}^{ext}] = \begin{bmatrix} G_{2D}^{ext}(\rho_{11}) & \dots & G_{2D}^{ext}(\rho_{1n}) & \dots & G_{2D}^{ext}(\rho_{1N}) \\ \dots & \dots & \dots & \dots & \dots \\ G_{2D}^{ext}(\rho_{m1}) & \dots & G_{2D}^{ext}(\rho_{mn}) & \dots & G_{2D}^{ext}(\rho_{mN}) \\ \dots & \dots & \dots & \dots & \dots \\ G_{2D}^{ext}(\rho_{M1}) & \dots & G_{2D}^{ext}(\rho_{Mn}) & \dots & G_{2D}^{ext}(\rho_{MN}) \end{bmatrix} \tag{19}$$

with size $M \times N$,

$$[\mathrm{Re}\left\{J_v^{mn}\right\}] = \begin{bmatrix} \mathrm{Re}\left\{J_v^{mn}(x_1,y_1)\right\} \\ \dots \\ \mathrm{Re}\left\{J_v^{mn}(x_n,y_n)\right\} \\ \dots \\ \mathrm{Re}\left\{J_v^{mn}(x_N,y_N)\right\} \end{bmatrix}, \quad [\mathrm{Im}\left\{J_v^{mn}\right\}] = \begin{bmatrix} \mathrm{Im}\left\{J_v^{mn}(x_1,y_1)\right\} \\ \dots \\ \mathrm{Im}\left\{J_v^{mn}(x_n,y_n)\right\} \\ \dots \\ \mathrm{Im}\left\{J_v^{mn}(x_N,y_N)\right\} \end{bmatrix} \tag{20}$$

with size $N \times 1$.

2 Legend

- ST-BCS is the single-task Bayesian Compressive Sampling-based technique
- MT-BCS-Jmn is the multi-task Bayesian Compressive Sampling-based technique that exploits the correlation between the real and imaginary parts of the source

3 Tests Dominio $L = 3.00\lambda$

3.1 TEST CASE: Two Square Cylinders $L = 0.16\lambda$

Goal: show the performances of BCS when dealing with a sparse scatterer

- Number of Views: V
- Number of Measurements: M
- Number of Cells for the Inversion: N
- Number of Cells for the Direct solver: D
- Side of the investigation domain: L

Test Case Description

Direct solver:

- Square domain divided in $\sqrt{D} \times \sqrt{D}$ cells
- Domain side: $L = 3\lambda$
- $D = 1296$ (discretization for the direct solver: $< \lambda/10$)

Investigation domain:

- Square domain divided in $\sqrt{N} \times \sqrt{N}$ cells
- $L = 3\lambda$
- $2ka = 2 \times \frac{2\pi}{\lambda} \times \frac{L\sqrt{2}}{2} = 6\pi\sqrt{2} = 26.65$
- $\#DOF = \frac{(2ka)^2}{2} = \frac{(2\times\frac{2\pi}{\lambda}\times\frac{L\sqrt{2}}{2})^2}{2} = 4\pi^2\left(\frac{L}{\lambda}\right)^2 = 4\pi^2 \times 9 \approx 355.3$
- N scelto in modo da essere vicino a $\#DOF$: $N = 324$ (18×18)

Measurement domain:

- Measurement points taken on a circle of radius $\rho = 3\lambda$
- Full-aspect measurements
- $M \approx 2ka \rightarrow M = 27$

Sources:

- Plane waves
- $V \approx 2ka \rightarrow V = 27$
- Amplitude: $A = 15.$
- Frequency: 300 MHz ($\lambda = 1$)

Object:

- Two square cylinders of side $\frac{\lambda}{6} = 0.1667$
- $\varepsilon_r \in \{1.5, 2.0, 2.5, 3.0, 3.5, 4.0, 4.5, 5.0\}$ (one square), $\varepsilon_r = 1.6$ (one square)
- $\sigma = 0$ [S/m]

MT-BCS-Jmn parameters:

- Gamma prior on noise variance parameter: $a = 5 \times 10^0$
- Gamma prior on noise variance parameter: $b = 8 \times 10^{-2}$
- Convergenze parameter: $\tau = 1.0 \times 10^{-8}$

RESULTS: Two Square Cylinders $L = 0.16\lambda$

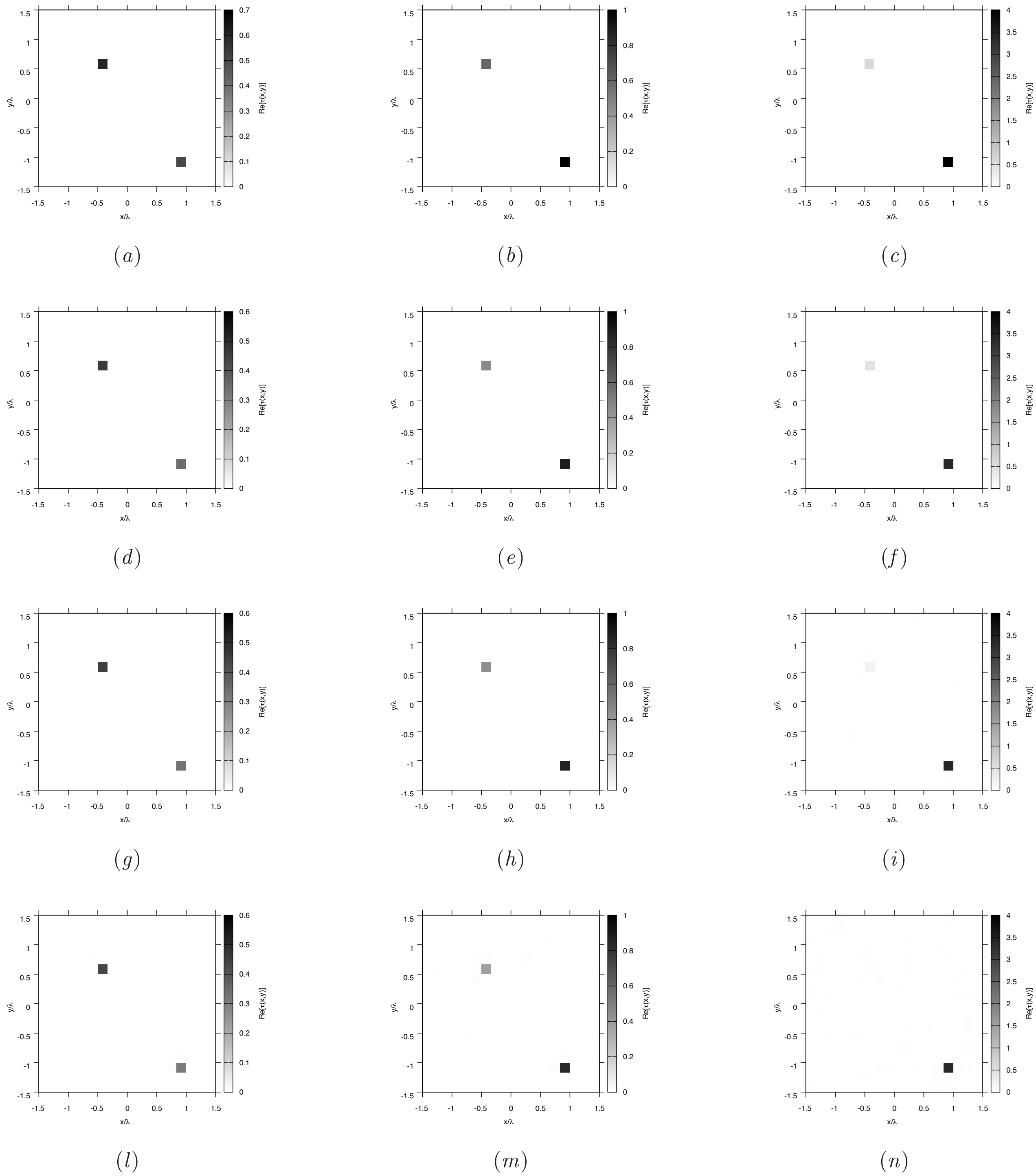

Figure 4. Actual object $(a)(b)(c)$ and MT-BCS-Jmn reconstructed object with $\varepsilon_r = 1.5$ $(d)(g)(l)$, $\varepsilon_r = 2.0$ $(e)(h)(m)$, and $\varepsilon_r = 5.0$ $(f)(i)(n)$, for Noiseless case $(d)(e)(f)$, $SNR = 10$ [dB] $(g)(h)(i)$ and $SNR = 5$ [dB] $(l)(m)(n)$.

RESULTS: Two Square Cylinders $L = 0.16\lambda$ - Error Figures - Comparison ST-BCS/MT-BCS

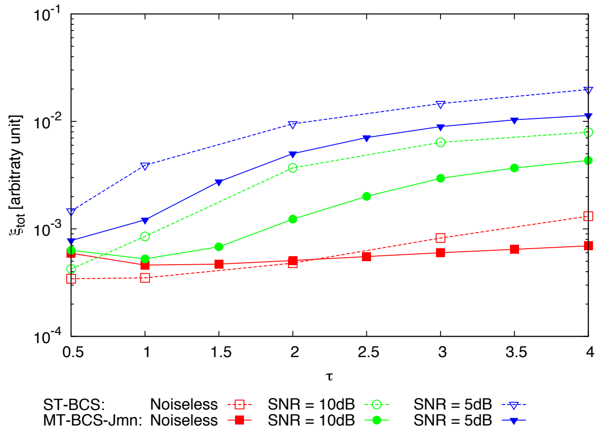

(a)

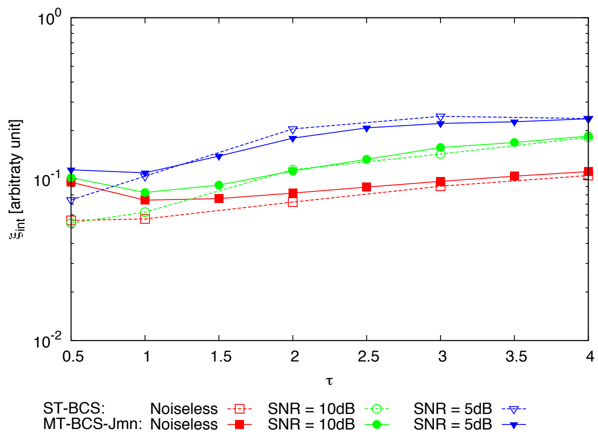

(b)

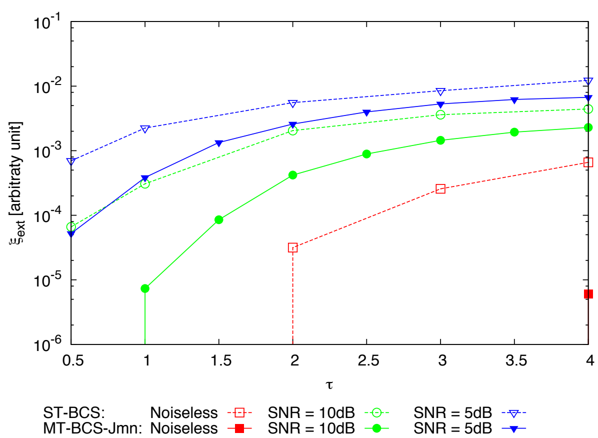

(c)

Figure 5. Behaviour of error figures as a function of ε_r, for different SNR values: (a) total error ξ_{tot}, (b) internal error ξ_{int}, (c) external error ξ_{ext}.

3.2 TEST CASE: Three Square Cylinders $L = 0.16\lambda$

Goal: show the performances of BCS when dealing with a sparse scatterer

- Number of Views: V
- Number of Measurements: M
- Number of Cells for the Inversion: N
- Number of Cells for the Direct solver: D
- Side of the investigation domain: L

Test Case Description

Direct solver:

- Square domain divided in $\sqrt{D} \times \sqrt{D}$ cells
- Domain side: $L = 3\lambda$
- $D = 1296$ (discretization for the direct solver: $< \lambda/10$)

Investigation domain:

- Square domain divided in $\sqrt{N} \times \sqrt{N}$ cells
- $L = 3\lambda$
- $2ka = 2 \times \frac{2\pi}{\lambda} \times \frac{L\sqrt{2}}{2} = 6\pi\sqrt{2} = 26.65$
- $\#DOF = \frac{(2ka)^2}{2} = \frac{(2\times\frac{2\pi}{\lambda}\times\frac{L\sqrt{2}}{2})^2}{2} = 4\pi^2\left(\frac{L}{\lambda}\right)^2 = 4\pi^2 \times 9 \approx 355.3$
- N scelto in modo da essere vicino a $\#DOF$: $N = 324$ (18×18)

Measurement domain:

- Measurement points taken on a circle of radius $\rho = 3\lambda$
- Full-aspect measurements
- $M \approx 2ka \rightarrow M = 27$

Sources:

- Plane waves
- $V \approx 2ka \rightarrow V = 27$
- Amplitude: $A = 1$
- Frequency: 300 MHz ($\lambda = 1$)

Object:

- Three square cylinders of side $\frac{\lambda}{6} = 0.1667$
- $\varepsilon_r \in \{1.5, 2.0, 2.5, 3.0, 3.5, 4.0, 4.5, 5.0\}$ (two square), $\varepsilon_r = 1.6$ (one square)
- $\sigma = 0$ [S/m]

MT-BCS-Jmn parameters:

- Gamma prior on noise variance parameter: $a = 5 \times 10^0$
- Gamma prior on noise variance parameter: $b = 8 \times 10^{-2}$
- Convergenze parameter: $\tau = 1.0 \times 10^{-8}$

RESULTS: Three Square Cylinders $L = 0.16\lambda$

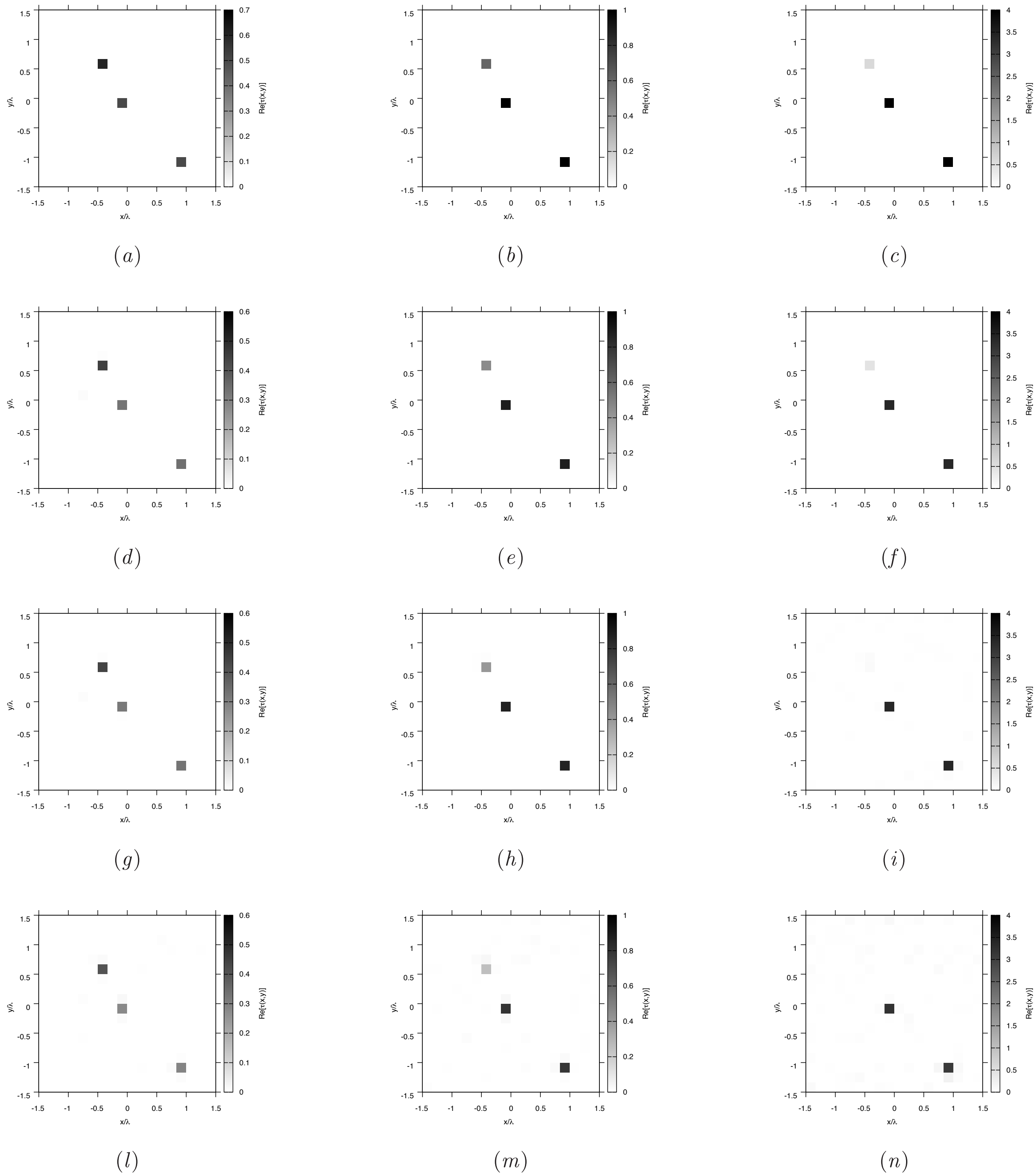

Figure 6. Actual object $(a)(b)(c)$ and MT-BCS-Jmn reconstructed object with $\varepsilon_r = 1.5$ $(d)(g)(l)$, $\varepsilon_r = 2.0$ $(e)(h)(m)$, and $\varepsilon_r = 5.0$ $(f)(i)(n)$, for Noiseless case $(d)(e)(f)$, $SNR = 10$ [dB] $(g)(h)(i)$ and $SNR = 5$ [dB] $(l)(m)(n)$.

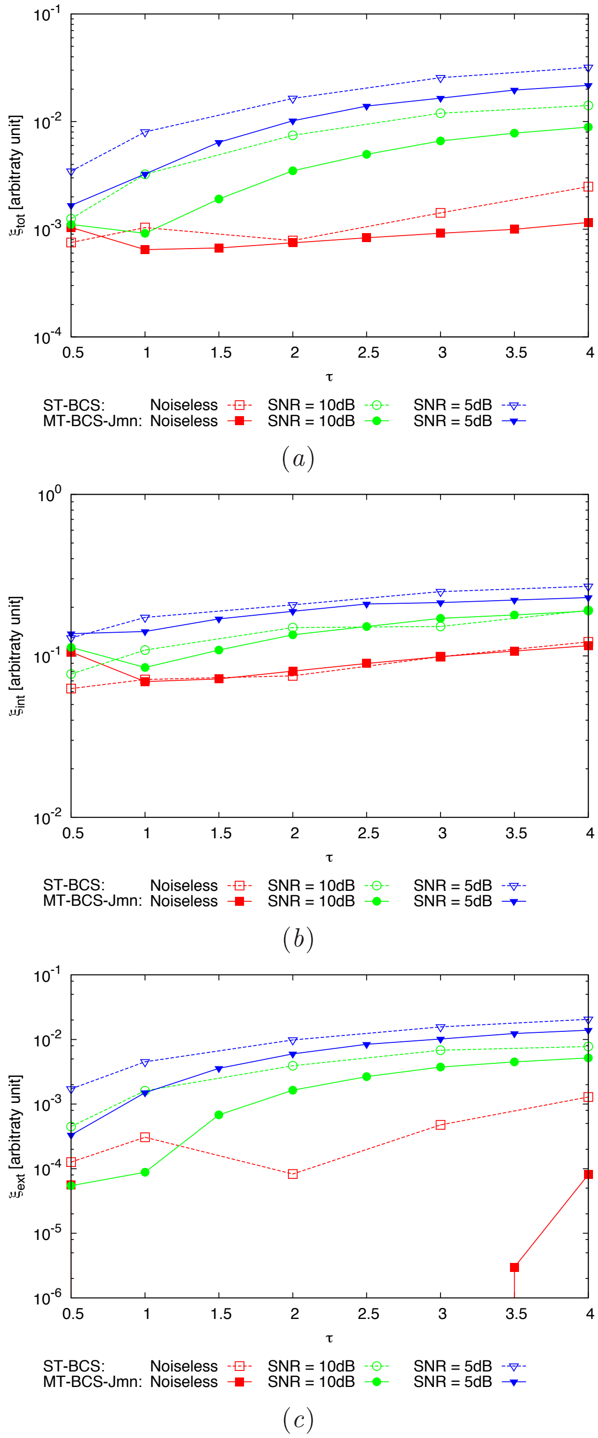

Figure 7. Behaviour of error figures as a function of ε_r, for different SNR values: (a) total error ξ_{tot}, (b) internal error ξ_{int}, (c) external error ξ_{ext}.

3.3 TEST CASE: Four Square Cylinders $L = 0.16\lambda$

Goal: show the performances of BCS when dealing with a sparse scatterer

- Number of Views: V
- Number of Measurements: M
- Number of Cells for the Inversion: N
- Number of Cells for the Direct solver: D
- Side of the investigation domain: L

Test Case Description

Direct solver:

- Square domain divided in $\sqrt{D} \times \sqrt{D}$ cells
- Domain side: $L = 3\lambda$
- $D = 1296$ (discretization for the direct solver: $< \lambda/10$)

Investigation domain:

- Square domain divided in $\sqrt{N} \times \sqrt{N}$ cells
- $L = 3\lambda$
- $2ka = 2 \times \frac{2\pi}{\lambda} \times \frac{L\sqrt{2}}{2} = 6\pi\sqrt{2} = 26.65$
- $\#DOF = \frac{(2ka)^2}{2} = \frac{(2\times\frac{2\pi}{\lambda}\times\frac{L\sqrt{2}}{2})^2}{2} = 4\pi^2\left(\frac{L}{\lambda}\right)^2 = 4\pi^2 \times 9 \approx 355.3$
- N scelto in modo da essere vicino a $\#DOF$: $N = 324$ (18×18)

Measurement domain:

- Measurement points taken on a circle of radius $\rho = 3\lambda$
- Full-aspect measurements
- $M \approx 2ka \rightarrow M = 27$

Sources:

- Plane waves
- $V \approx 2ka \rightarrow V = 27$
- Amplitude: $A = 1$
- Frequency: 300 MHz ($\lambda = 1$)

Object:

- Four square cylinders of side $\frac{\lambda}{6} = 0.1667$
- $\varepsilon_r \in \{1.5, 2.0, 2.5, 3.0, 3.5, 4.0, 4.5, 5.0\}$ (two square), $\varepsilon_r = 1.6$ (two square)
- $\sigma = 0$ [S/m]

MT-BCS-Jmn parameters:

- Gamma prior on noise variance parameter: $a = 5 \times 10^0$
- Gamma prior on noise variance parameter: $b = 8 \times 10^{-2}$
- Convergenze parameter: $\tau = 1.0 \times 10^{-8}$

RESULTS: Four Square Cylinders $L = 0.16\lambda$

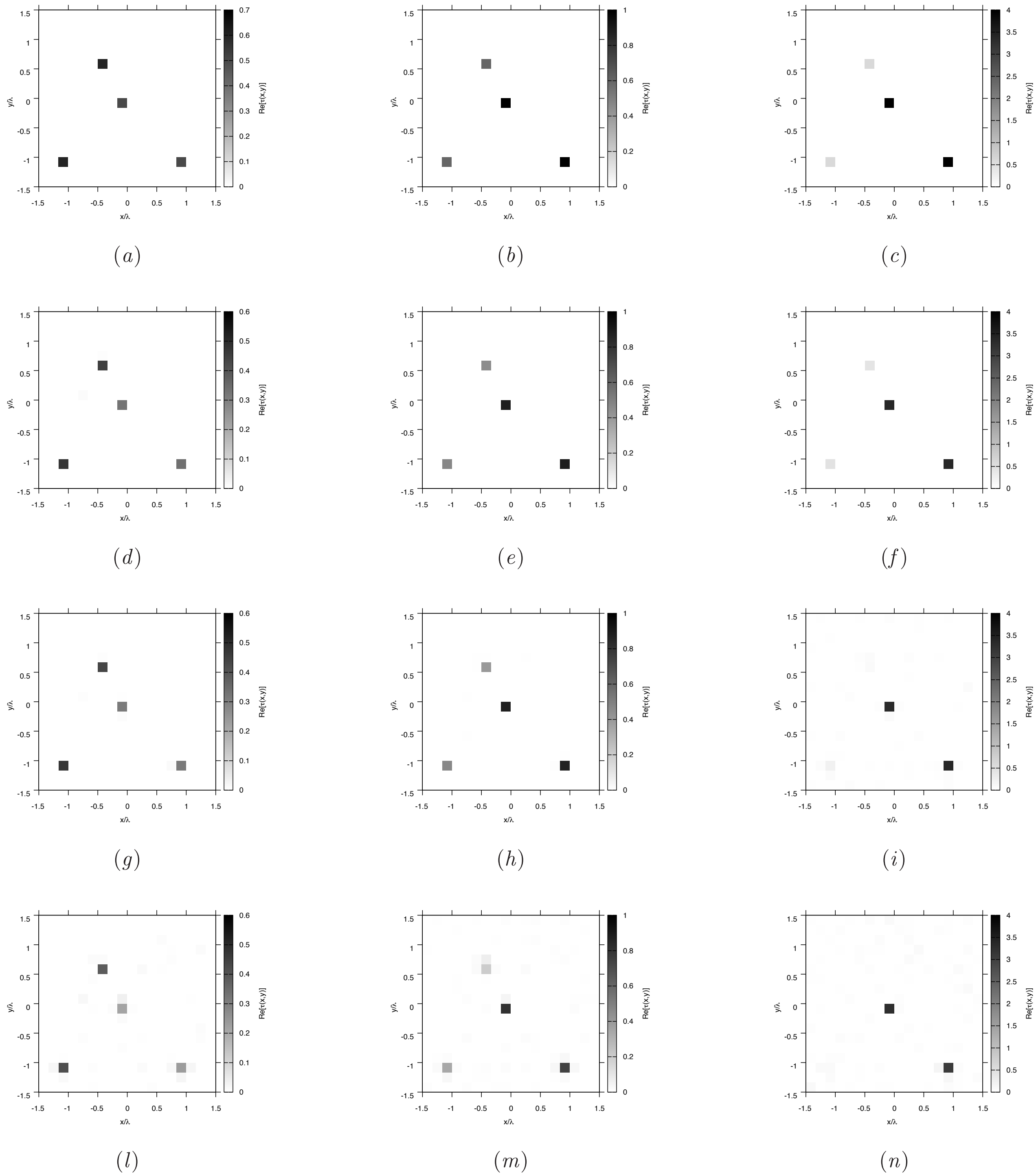

Figure 8. Actual object $(a)(b)(c)$ and MT-BCS-Jmn reconstructed object with $\varepsilon_r = 1.5$ $(d)(g)(l)$, $\varepsilon_r = 2.0$ $(e)(h)(m)$, and $\varepsilon_r = 5.0$ $(f)(i)(n)$, for Noiseless case $(d)(e)(f)$, $SNR = 10$ [dB] $(g)(h)(i)$ and $SNR = 5$ [dB] $(l)(m)(n)$.

RESULTS: Four Square Cylinders $L = 0.16\lambda$ - Error Figures - Comparison ST-BCS/MT-BCS

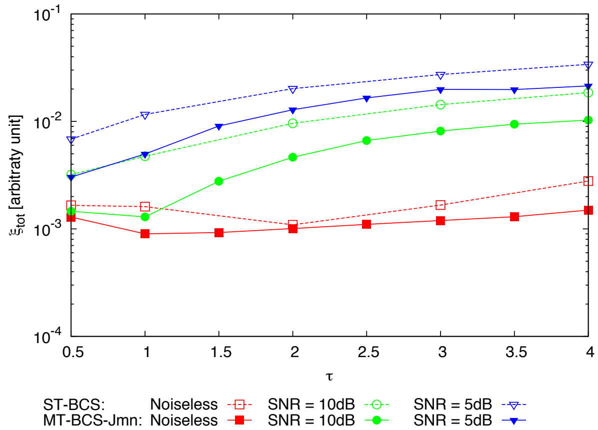

(a)

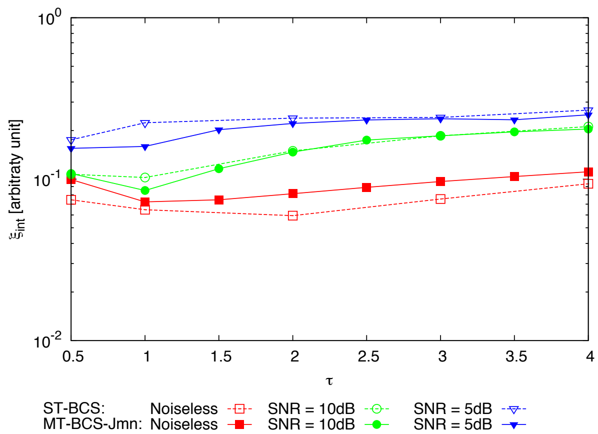

(b)

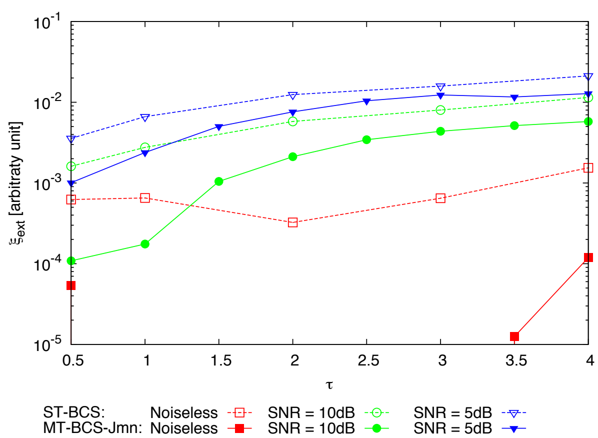

(c)

Figure 9. Behaviour of error figures as a function of ε_r, for different SNR values: (a) total error ξ_{tot}, (b) internal error ξ_{int}, (c) external error ξ_{ext}.

References

[1] G. Oliveri, N. Anselmi, and A. Massa, "Compressive sensing imaging of non-sparse 2D scatterers by a total-variation approach within the Born approximation," IEEE Trans. Antennas Propag., vol. 62, no. 10, pp. 5157-5170, Oct. 2014.

[2] L. Poli, G. Oliveri, and A. Massa, "Imaging sparse metallic cylinders through a Local Shape Function Bayesian Compressive Sensing approach," Journal of Optical Society of America A, vol. 30, no. 6, pp. 1261-1272, 2013.

[3] L. Poli, G. Oliveri, P. Rocca, and A. Massa, "Bayesian compressive sensing approaches for the reconstruction of two-dimensional sparse scatterers under TE illumination," IEEE Trans. Geosci. Remote Sensing, vol. 51, no. 5, pp. 2920-2936, May. 2013.

[4] L. Poli, G. Oliveri, and A. Massa, "Microwave imaging within the first-order Born approximation by means of the contrast-field Bayesian compressive sensing," IEEE Trans. Antennas Propag., vol. 60, no. 6, pp. 2865-2879, Jun. 2012.

[5] G. Oliveri, P. Rocca, and A. Massa, "A bayesian compressive sampling-based inversion for imaging sparse scatterers," IEEE Trans. Geosci. Remote Sensing, vol. 49, no. 10, pp. 3993-4006, Oct. 2011.

[6] G. Oliveri, L. Poli, P. Rocca, and A. Massa, "Bayesian compressive optical imaging within the Rytov approximation," Optics Letters, vol. 37, no. 10, pp. 1760-1762, 2012.

[7] P. Rocca, M. Carlin, L. Manica, and A. Massa, "Microwave imaging within the interval analysis framework," Progress in Electromagnetic Research, vol. 143, pp. 675-08, 2013.

[8] P. Rocca, M. Carlin, G. Oliveri, and A. Massa, "Interval analysis as applied to inverse scattering," IEEE International Symposium on Antennas Propag. (APS/URSI 2013), Chicago, Illinois, USA, Jul. 8-14, 2012.

[9] P. Rocca, M. Carlin, and A. Massa, "Imaging weak scatterers by means of an innovative inverse scattering technique based on the interval analysis," 6th European Conference on Antennas Propag. (EuCAP 2012), Prague, Czech Republic, Mar. 26-30, 2012.

[10] G. Oliveri and A. Massa, "Bayesian compressive sampling for pattern synthesis with maximally sparse non-uniform linear arrays," IEEE Trans. Antennas Propag., vol. 59, no. 2, pp. 467-481, Feb. 2011.

[11] G. Oliveri, M. Carlin, and A. Massa, "Complex-weight sparse linear array synthesis by Bayesian Compressive Sampling," IEEE Trans. Antennas Propag., vol. 60, no. 5, pp. 2309-2326, May 2012.

[12] F. Viani, G. Oliveri, and A. Massa, "Compressive sensing pattern matching techniques for synthesizing planar sparse arrays," IEEE Trans. Antennas Propag., vol. 61, no. 9, pp. 4577-4587, Sept. 2013.